2016 NDIA GROUND VEHICLE SYSTEMS ENGINEERING AND TECHNOLOGY SYMPOSIUM
VEHICLE ELECTRONICS AND ARCHITECTURE (VEA) TECHNICAL SESSION
AUGUST 2-4, 2016 – NOVI, MICHIGAN

AN IMPROVED WAVEGUIDE MODEL TO SUPPORT ANALYSIS OF ELECTROMAGNETIC SHIELDING FOR LIQUID COOLED POWER ELECTRONICS

Scott W. Faust
U.S. Army Tank Automotive Research, Development, and Engineering Center (TARDEC)
Warren, MI

ABSTRACT

This paper describes ongoing work to develop and validate an improved waveguide model in order to support analysis of shielding effectiveness at frequencies from 8 GHz to 25 GHz. Waveguides may be used in the coolant loop for liquid-cooled, high-voltage power electronics to maintain the shielding effectiveness of the enclosure surrounding the power electronics. Different formulas for shielding effectiveness are reviewed and their applicability and limitations examined. The improved model is then used to predict the shielding effectiveness of an air-filled waveguide with a hexagonal or "honeycomb" insert installed. The results obtained are then compared with results obtained by modeling and simulation using FEKO.

INTRODUCTION

As the U.S. Army conducts research into hybrid powertrains for future Military Ground Vehicles, high voltage (HV), high power-density electronic modules are increasingly being used to meet Size, Weight, Power, and Cooling (SWAP-C) requirements. The maximum allowable junction temperatures of the electronic components (e.g., insulated gate bipolar transistors or IGBTs) associated with these modules (controllers, inverters, DC/DC converters, etc.) varies based on the underlying component technology [1]. The upper limit on junction temperature for semiconductors ranges from +150°C for silicon to +200°C for silicon carbide.

Regardless of the component technology selected, these modules are required to dissipate a significant amount of heat to maintain the junction temperature below these maximums. This is even more critical for high power components such as a high-voltage integrated starter generator which may provide up to 160 kW of power [2]. The use of convection cooling to remove excess heat from these components quickly reaches a diminishing point of return as air is a poor conductor of heat when compared to liquids [3]. The end result is an increasing reliance on liquid cooling to obtain the required heat transfer [1]. This presents a challenge to test and evaluation (T&E) engineers in the evaluation of these subsystems for electromagnetic interference (EMI).

Current Military Standards (MIL-STD) mandate the use of a shielded enclosure to create an electromagnetically quiet environment for the testing of these subsystems [4] [5]. This prevents the surrounding electromagnetic environment from interfering with the measurement of emissions, prevents radio frequency (RF) energy generated within the enclosure during susceptibility testing from interfering with other users of the electromagnetic spectrum, and protects individuals performing susceptibility testing from the hazards of electromagnetic radiation to personnel, or HERP. The ability of the enclosure to perform these tasks is expressed as the shielding effectiveness (SE) of the enclosure. The requirement for liquid cooling of these systems during testing requires penetrations through the boundary of the shielded enclosure. These penetrations present potential coupling paths for interference to enter the enclosure and leakage of RF into the surrounding environment. For liquid coolants, waveguides provide a convenient solution to this problem.

The use of waveguides maintains the SE of the enclosure when testing power electronics by allowing for circulation of liquid coolants into and out of the

enclosure. Circular waveguides provide a convenient means by being mechanically compatible with existing standard plumbing sizes. Selection of a waveguide having the desired SE for the expected frequency range, however, is complicated by the need to select a workable model from different sources, each having varying degrees of completeness, and not all of them in agreement.

Prior work by Chen (1972) provided formulas to rapidly calculate the SE of a thick plate perforated by various geometric arrangements of circular and square apertures by solving for the reflection and transmission coefficients at the apertures [6]. McInerny et al. (1984) characterized fluid-filled waveguides over a limited frequency range, and proposed the contribution of multiple, smaller waveguides in parallel within a larger waveguide to SE as being the attenuation of a single insert. Calculation of the attenuation of a waveguide with multiple inserts was limited to a brief discussion of the results obtained from a computer program, and no model or formula presented for this particular configuration [7]. Hemming (1992) discussed the cutoff frequency of an individual waveguide, the reduction in this cutoff frequency related to the dielectric constant of the material or media within the waveguide, and an estimate of the SE of a "honeycomb insert" being proportional to the dimensions of an individual insert and the number of inserts [8]. Lee et al. (2005) provided a model of the shielding effectiveness of a single honeycomb insert, with adjustments to the original equation to improve consistency with the results of simulation [9]. Industry literature quotes the SE of a simple waveguide, with references to the availability of a honeycomb insert to increase the cutoff frequency [10].

This paper proposes an improved model for determining the SE of a waveguide with a honeycomb insert by addressing the relationship between the number of inserts and the dielectric constant of the coolant; reviewing the different theoretical models proposed for a honeycomb insert; and comparing the theoretical results to those obtained by simulation.

WHAT IS SHIELDING EFFECTIVENESS?

According to IEEE Std 299™-2006, the shielding effectiveness (SE) of a shielded enclosure is calculated as the ratio of two electromagnetic field measurements. Depending on the frequency range of interest, the electric/magnetic field or the associated power may be measured. The first measurement is performed with no shielding material present. The second measurement is performed with the shielding material in between the two antennas. If the electric

field is measured, the SE is calculated as the ratio of the two measurements in decibels [11], or

$$SE_E = -20 \log_{10} \left(\frac{E_{transmitted}}{E_{incident}} \right) \quad (1).$$

The SE of the enclosure is reduced by conductors which pass through the walls of the enclosure, and by the presence of openings, or apertures, in the shielded enclosure itself. It is the latter upon which this paper will focus, specifically the presence of waveguides and their impact on shielding effectiveness.

SHIELDING EFFECTIVENESS OF A WAVEGUIDE

The SE of a waveguide at any given frequency is determined by the coupling of the incident electromagnetic wave to the opening of the waveguide [9], and the relationship between the physical dimensions, the material within, and the frequency of the electromagnetic wave passing through the waveguide [12]. The inclusion of a honeycomb insert will also improve the SE of the waveguide.

Coupling of an Incident Wave to the Opening of the Waveguide

At the opening of the waveguide, the electromagnetic wave makes the transition from the outside world to the inside of the waveguide. This occurs when an electromagnetic wave is:

- Incident upon the opening of the waveguide, either with the direction of propagation perpendicular to the opening (normal incidence) or at a non-zero *angle of incidence* with respect to the longitudinal axis of the waveguide (oblique incidence).
- Directly coupled into the waveguide, as the continuation of a connection from another waveguide or a feed point.

An example of the first situation is an uncapped waveguide on an enclosure where a plane wave in free space outside the enclosure is incident on the opening and couples into the waveguide. Examples of the second situation are a waveguide having an external connection to an external source, be it another waveguide or a non-conductive coolant line.

Wave Propagation through the Waveguide

In setting out to provide a model for the SE of a circular waveguide, some conventions must first be established. In a circular waveguide, the cylindrical coordinate system (ρ, ϕ, z) is commonly used to uniquely define points within the waveguide with the *z*-axis oriented along the length of the waveguide. The direction of propagation through the waveguide is in

the positive direction along the *z*-axis. A detailed description of solutions to the wave equation for the various modes of propagation is beyond the scope of this paper and is provided in [12]; however, it is important to note that solutions to the wave equation involve an exponential term indicative of propagation through the waveguide. For the +*z* direction, this exponential term is of the form

$$e^{-(\alpha_t + j\beta_z)z} \qquad (2).$$

Equation (2) may be used to determine the SE of a waveguide below the cutoff frequency by calculating the attenuation of the wave along the length of the waveguide. The term α_t is the sum of conductive losses α_c (waveguide material) and dielectric losses α_d (coolant) is

$$\alpha_t = \alpha_c + \alpha_d \qquad (3)$$

and is typically stated in units of decibels per meter or kilometer [12].

Below the cutoff frequency, the propagation constant β_z is imaginary; there is no propagation through the waveguide. Above the cutoff frequency, the propagation constant is real, and in equation (2) represents the phase change of the electromagnetic wave.

SE and Cutoff Frequency

This section will discuss the shielding effectiveness of a circular waveguide in terms of a *cutoff frequency* (*f$_c$*). Every waveguide has a cutoff frequency, above which the electromagnetic wave travels or propagates through the waveguide with minimum attenuation. Below this cutoff frequency, the electromagnetic wave is rapidly attenuated. The cutoff frequency is derived from solutions to the wave equation constructed from Maxwell's Equations, and the boundary conditions of the waveguide, and expressed with respect to the *mode of propagation* for the electric and magnetic fields within the waveguide [12]. The dominant mode of propagation, or *transverse electric* (TE$_{11}$) will be considered, as the solution to the wave equation for this mode results in the lowest cutoff frequency of the waveguide. In addition, when calculating *f$_c$* for a given waveguide configuration, this paper will consider the waveguide to be completely filled with whatever material is being passed through the waveguide. If the waveguide is only partially filled i.e., incomplete coverage of the cross-sectional area of the waveguide, or multiple layers of different material through the waveguide, the solution to the wave equation increases in complexity.

The cutoff frequency *f$_c$* of any waveguide, rectangular or circular, is dependent on the cross-sectional dimensions of the waveguide and the constitutive parameters of the material within the waveguide. For a circular waveguide, the dimension of interest is the radius. The constitutive parameters used to calculate the cutoff frequency are the permeability μ and permittivity ε. The cutoff frequency for the dominant mode of propagation TE$_{11}$ is [12]

$$f_c = \frac{\chi'_{11}}{2\pi a \sqrt{\mu\varepsilon}} \qquad (4)$$

where *a* is the radius of the waveguide in meters,

$$\chi'_{11} = 1.8412 \qquad (5)$$

$$\mu = \mu_r \mu_0 \qquad (6)$$

$$\varepsilon = \varepsilon_r \varepsilon_0 \qquad (7)$$

The value of χ'_{11} in (4) is a zero of the derivative of the Bessel function $J'_m(\chi'_{mn}) = 0$. This and other values for χ'_{mn} are tabulated and readily available in various mathematical reference books [13]. The permeability of free space,

$$\mu_0 = 4\pi \times 10^{-7} (henries/meter) \qquad (8)$$

and permittivity of free space,

$$\varepsilon_0 = 8.854 \times 10^{-12} (farads/meter) \qquad (9)$$

the relative permeability μ_r, and relative permittivity ε_r of the media in equation (3) are used to calculate *f$_c$*. In order to simplify the discussion, the material within the waveguide will be considered to be non-magnetic so the relative permeability will be unity ($\mu_r = 1$). In addition, the variation of ε with respect to frequency will not be considered. The constitutive properties of the material also determine the intrinsic impedance η (eta) of the material within the waveguide, expressed in ohms as

$$\eta = \sqrt{\frac{\mu}{\varepsilon}} \qquad (10).$$

For the TE$_{11}$ mode, below the cutoff frequency the phase constant in the direction of propagation is imaginary [12]

$$(\beta_z)_{11} = -j\beta \sqrt{\left(\frac{f_c}{f}\right)^2 - 1} \qquad (11).$$

Substitution of equation (11) into equation (2) with $\alpha_c = 0$ results in the calculation of a real number for the attenuation of the electromagnetic wave over a given distance *z*. The phase constant β in (11) is dependent on the frequency of the electromagnetic wave (not the cutoff frequency of the waveguide!) and the constitutive properties of the material within the

waveguide independent of the direction of propagation. It is calculated as

$$\beta = 2\pi f\sqrt{\mu\varepsilon} \qquad (12).$$

Substitution of equations (11, 12) into equation (2) for the TE_{11} mode below the cutoff frequency, converting the resulting expression to decibels, and treating attenuation as a positive number yields:

$$A = 54.58fL\left[\mu\varepsilon\left(\left(\frac{f_c}{f}\right)^2 - 1\right)\right]^{\frac{1}{2}} \qquad (13)$$

where f is the operating frequency (Hertz) below the cutoff frequency f_c of the waveguide, and L is the length of the waveguide (meters). A search of relevant literature [8] [14] [15] provides comparable equations for calculating the attenuation of a circular waveguide as a function of waveguide length. Equation (13) forms the basis for calculating the SE of the waveguide.

When a waveguide is filled with different materials, the constitutive parameters μ and ε change and affect both the cutoff frequency and SE of the waveguide. This is shown in Figure 1 for a circular waveguide of length L and fixed diameter D of one inch, and a ratio $R=L/D=5$. The material within the waveguide is considered to be non-magnetic i.e., $\mu_r=1$.
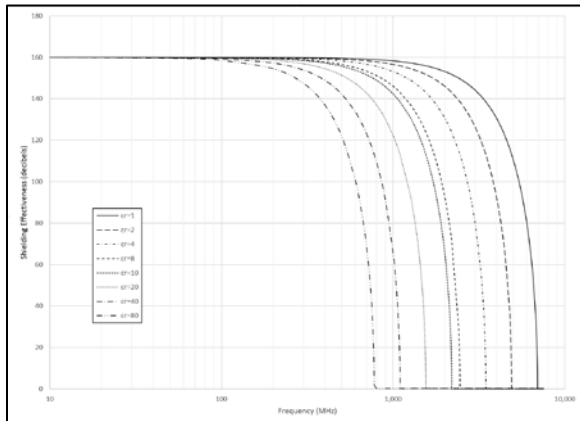

Figure 1 Comparison of SE for a waveguide filled with materials having different dielectric constants.

The permittivity ε of the material in the waveguide is proportional to the dielectric constant ε_r. In equation (13), as ε_r increases the cutoff frequency f_c decreases at a much faster rate, resulting in an overall decrease in SE as the operating frequency increases. Table 1 provides the relative dielectric constant for different materials, including two used as liquid coolants.

Table 1 Relative Dielectric Constants for Various Materials

Material	Relative Dielectric Constant ε_r
Air	~1
Ethylene Glycol [16]	41.4
Distilled Water [7]	59.6 – 76.8

SE and Honeycomb Insert

A waveguide may also contain an insert consisting of multiple, smaller waveguides e.g., a honeycomb insert as shown in Figure 2.
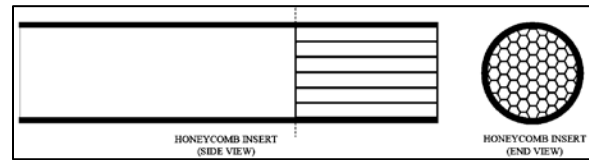

Figure 2 Waveguide with honeycomb insert.

The use of this honeycomb insert within the larger waveguide subdivides the overall cross-sectional area of the larger waveguide into many smaller waveguides. This insert increases the cutoff frequency of the overall waveguide because each individual smaller waveguide inherently has a higher cutoff frequency, which serves to maintain the required level of SE. This is important in situations where the larger waveguide is required to achieve a specified fluid flow rate, yet maintain a high level of SE when filled with various fluids. The sizing of the honeycomb insert is critical to maintaining the SE of the overall waveguide, both in cross-sectional area and length.

Estimating the Required Number of Honeycomb Inserts

To determine the required cross-sectional area of a single honeycomb insert, the cutoff frequency f_c of the original, unloaded waveguide is used to calculate the cross-sectional area of a waveguide having an equal cutoff frequency when loaded with the liquid coolant. For a given waveguide radius a, and treating the liquid coolant as non-magnetic i.e., $\mu_r = 1$ the radius a_L of the loaded waveguide will be smaller

$$a_L = \frac{a}{\sqrt{\varepsilon_r}} \qquad (14).$$

Equation (14) represents an upper limit on the radius of a single insert. To simplify calculation of the cutoff frequency and attenuation of a single honeycomb insert, the cross-sectional area of single hexagon of the honeycomb waveguide insert is approximated by a circle as shown in Figure 3.
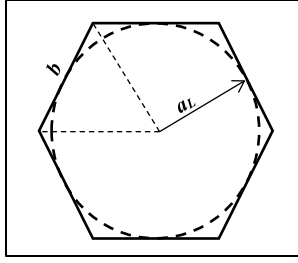
Figure 3 Circle approximation for the cross-section of a single honeycomb waveguide insert.

By setting the radius of the inscribed circle equal to a_L, this approximation provides a method to quickly determine the maximum permitted dimension b of the honeycomb insert:

$$b = \frac{2\sqrt{3}}{3} a_L = \frac{2}{3} \sqrt{\frac{3}{\varepsilon_r}} a \qquad (15).$$

The cutoff frequency and attenuation of an individual insert in decibels may then be calculated by using a_L in equations (3,12), respectively.

The minimum number of inserts N required to achieve an equivalent cross-sectional area for flow and maintain the SE is related to the dielectric constant of the coolant by

$$N \geq \varepsilon_r \qquad (16).$$

Hemming (1992) provided an estimate for the SE of a honeycomb vent as [8]

$$A(dB) = 27 \frac{L_{insert}}{a_L} - 20 \log_{10} N \qquad (17)$$

which results in a decrease in SE as the number of inserts N increases, i.e., the surface area covered by the honeycomb structure is increasing. In contrast, Kaiser (2006) proposed the use of a honeycomb structure, consisting of N waveguides with the equivalent cross-sectional area of a single larger waveguide, improves the SE of the original waveguide by [17]

$$10 \log_{10} N \qquad (18).$$

Equation (18) holds true only if the diameter of a single insert is much smaller than the wavelength of the electromagnetic wave within the larger waveguide. The commonly accepted value of "electrically small" is 1/10 of wavelength [18]. For equation (18) to apply,

$$2a_L < \frac{\lambda}{10} \qquad (19).$$

The SE of the insert at operating frequencies above the cutoff frequency f_c of the larger waveguide, and below the cutoff frequency $f_{c,insert}$ of an individual insert may then be calculated from the cross-sectional area of an individual insert and the number of inserts.

PROPOSED IMPROVED WAVEGUIDE MODEL FORMULAS

It is proposed the SE below the cutoff frequency of a waveguide with a honeycomb insert may be modeled in two parts. Referring back to Figure 2, the first part of the waveguide is the larger waveguide surrounding the insert. The second part is the honeycomb insert itself.

SE Below f_c, All Models

At frequencies below f_c of the large waveguide i.e., $f < f_c$ the SE is

$$SE = 54.58 f L \left[\mu \varepsilon \left(\left(\frac{f_c}{f} \right)^2 - 1 \right) \right]^{\frac{1}{2}} + SE_n \quad (20)$$

where SE_n represents the SE of the nth model or case. At frequencies greater than the cutoff frequency of the larger waveguide, yet below the frequency where the diameter of a single honeycomb insert, three different cases were considered.

SE Above f_c, Below $f_{c,insert}$, Case 1 (SE_1)

The first approach incorporates equation (18) to calculate SE as the combination of a single insert and the contribution of subdividing the cross-sectional area of the larger waveguide into N smaller waveguides

$$SE_1 \cong 10 \log_{10} N$$

$$+54.58 f L_{insert} \left[\mu \varepsilon \left(\left(\frac{f_{c,insert}}{f} \right)^2 - 1 \right) \right]^{\frac{1}{2}} \qquad (21).$$

The circular approximation of radius a_L for a honeycomb insert is used as the basis or $f_{c,insert}$. In this approach, the right hand side of equation (18) is tested for both $\lambda/10$ and $\lambda/5$.

SE Above f_c, Below $f_{c,insert}$, Case 2 (SE_2)

Chen (1973) provides a series of equations to calculate the SE of an arrangement of a panel with circular apertures located at the vertices of an equilateral triangle [6]. The transmission coefficient

$$T = \frac{1}{1 - j[A + B \tanh(\beta L_{insert})]} - \frac{1}{1 - j[A + B \coth(\beta L_{insert})]} \quad (22)$$

where:

$$A = 12 \left(\frac{4}{3} \left(\frac{\lambda}{2a_L} \right)^2 - 1 \right)^{1/2} \left[\frac{J_1'\left(\frac{2\pi}{\sqrt{3}} \right)}{1 - \left(\frac{8\pi}{1.841\sqrt{3}} \right)^2} \right]^2 -$$

$$\frac{12}{\left(\frac{4}{3} \left(\frac{\lambda}{2a_L} \right)^2 - 1 \right)^{1/2}} \left[\frac{J_1'\left(\frac{2\pi}{\sqrt{3}} \right)}{\frac{2\pi}{\sqrt{3}}} \right]^2 \qquad (23)$$

$$B = 1.32 \left(\left(\frac{0.293\lambda}{a_L} \right)^2 - 1 \right)^{1/2} \tag{24}$$

$$\beta = \frac{2\pi}{\lambda} \left(\left(\frac{0.293\lambda}{a_L} \right)^2 - 1 \right)^{1/2} \tag{25}$$

and T is used to calculate the SE of the insert for TE_{11} polarization

$$SE_2 = -20 \log_{10} \left| (T \cos \theta)^{2(1-p)} \right| \tag{26}$$

with p defined as a percentage related to the porosity of the surface, and angle of incidence $\theta = 0$ degrees or normal incidence. As in Case 1, the circular approximation of a honeycomb insert was used to calculate $f_{c,insert}$. Chen reports the solution obtained by this method has an uncertainty of ± 1.5 dB for angles of incidence $\theta < 60°$ [6].

SE Above f_c, Below $f_{c,insert}$, Case 3 (SE_3)

Lee et al. (2005) propose the SE for a honeycomb insert to be the contribution of a single insert [9]

$$SE_3 = 17.5 \frac{L_{insert\,[mm]}}{b_{[mm]}} \sqrt{1 - \left(\frac{b_{[mm]} f_{[MHz]}}{96659} \right)^2} - 20 \log_{10} \left(\frac{2\beta b_{[mm]}}{\pi} \cos \theta \right) - 20 \log_{10} \left(\frac{2Rb}{f_{[MHz]}} \right) \tag{27}$$

where $R = 3.18/b$ and θ is the angle of incidence with respect to the longitudinal axis of the waveguide. The third term is only added if

$$\frac{f_c}{f} > 5R \tag{28}.$$

Bereuter and Chang (1982) indicate the second term of equation (27) is valid only if [19]

$$\beta a_L \leq 0.5 \tag{29}.$$

In calculating the contribution of SE_3 to equation (19), these conditions were taken into account.

SE Above $f_{c,insert}$

Recalling equation (3), the SE of the waveguide is dependent on α_t at frequencies greater than the cutoff frequency of the insert. The contribution from the conductor and dielectric (coolant) losses for the TE_{11} mode of propagation [12] is

$$\alpha_c \cong 8.686 \frac{R_s}{a_L \eta \sqrt{1 - \left(\frac{f_{c,insert}}{f} \right)^2}}$$

$$\times \left[\left(\frac{f_{c,insert}}{f} \right)^2 - 0.4184 \right], f > f_{c,insert} \tag{30}$$

$$\alpha_d \cong \frac{27.27 \lambda_g}{\lambda^2} \tan \delta_e \tag{31}$$

where $\tan \delta_e$ is the loss tangent of the material. Equations (30-31) are in units of decibels per meter.

MODELING AND SIMULATION IN FEKO

Models were developed using Altair® HyperWorks® FEKO[1] software to analyze the SE of various waveguides, both open and with a finite number of inserts installed. In all models, an excitation port is located at one end of the waveguide, and the other end is terminated in a matching impedance. FEKO considers any port not connected to a source to be terminated in a matched impedance.

The longitudinal axis of the waveguide was oriented with respect to the chosen coordinate system such that the direction of propagation through the waveguide is in the +z direction. All metallic structures were modeled as Perfect Electric Conductor (PEC), and the material within the waveguide was considered to be free space i.e., $\mu_r = \varepsilon_r = 1$. For a waveguide constructed of PEC, $R_s = 0$ and $\tan \delta_e = 0$ for free space, resulting in $\alpha_t = 0$.

FEKO Solution Method Configuration

FEKO was configured to use the finite element method (FEM) to obtain solutions to the differential form of Maxwell's Equations. The Method of Moments (MoM) was decoupled from the FEM solution method. During each simulation, an S-parameter analysis of each waveguide model was performed to determine the SE by driving one port of the waveguide and examining the output at the opposite port i.e., S_{21}.

Simple Waveguide Model

The first model is a simple waveguide of radius $a = 12.7$ mm, and length to diameter ratio $R = 5$. The media inside the waveguide is free space. FEKO was configured to generate a "coarse" mesh based on the highest frequency requested in the simulation. This results in a mesh size of $\lambda/6$ [20]. The FEKO model is shown in Figure 4.

---

[1] FEKO is a German acronym for "FEldberechnung bei Körpern mit beliebigen Oberfläche," or in English "Field computations involving bodies of arbitrary shape." [20]
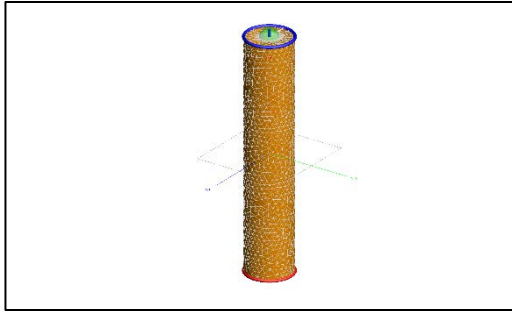
Figure 4 Simple waveguide model

Waveguide Model with Honeycomb Insert

The second model is a waveguide with a honeycomb insert installed. To create the model, the number of smaller circular inserts required was considered with the following goals in mind:

- Minimize the number of inserts used.
- Maximize the total cross-sectional area of the inserts as compared to the larger waveguide.
- Reduce the overall complexity of the model.
- Simplify calculation of the cutoff frequency and attenuation of an individual insert.

The optimal number of circles was determined to be seven based on a review of optimal packings of individual circles within a larger circle [21]. This results in each individual honeycomb insert having a radius of

$$a_L = \frac{a}{3} = 4.2333 \text{ mm} \qquad (32).$$

Using the circle approximation as shown in Figure 3 and equation (15), the maximum dimension of a single honeycomb insert is b=4.8882 mm. The ratio of length to diameter for the insert was set to integer multiples of b. The FEKO model for the waveguide with honeycomb insert is shown in Figure 5.
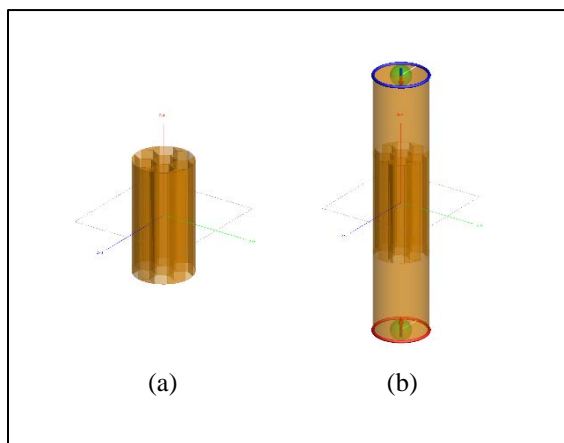

(a)   (b)

Figure 5 (a) Model of honeycomb insert with L_{insert}=5b, and (b) model of waveguide with honeycomb insert (a) installed

COMPARISON OF THEORETICAL AND SIMULATION RESULTS

Calculations of the theoretical attenuation for the base waveguide and honeycomb inserts were performed. The calculated results were then compared to those obtained from simulation using FEKO.

Basic Waveguide Parameters of Interest

The theoretical values for various parameters of the main waveguide and a single honeycomb insert are given in Table 2. The circle approximation shown in Figure 3 was used in order to utilize equation (4) when calculating the cutoff frequency for the insert.

Table 2 Waveguide Parameters

Parameter	Main WG	Single Insert
Radius (mm)	12.7	4.233
Length (mm)	127	9.776
f_c (GHz)	6.922	20.7665
Number of Inserts Within Main WG	--	7

Table 3 shows the relationship between the ratio of the length to diameter of the waveguide and the SE of the waveguide. The circle approximation shown in Figure 3 permits equation (13) to be used when calculating the SE for the insert. The values shown in Table 2 were used as the basis for D and L. Calculations for both the main waveguide and a single honeycomb insert are given.

Table 3 Theoretical Shielding Effectiveness of Circular Waveguide vs. Ratio of Length to Diameter at f=5 GHz

$R=L/D$	Main WG	Single Insert
1	22.12	31.04
2	44.24	62.09
3	66.36	93.13
4	88.48	124.18
5	110.60	155.22

Numerical Results and Discussion

A comparison of the theoretical SE calculated for each case, and modeling and simulation in FEKO is shown in Figure 6.
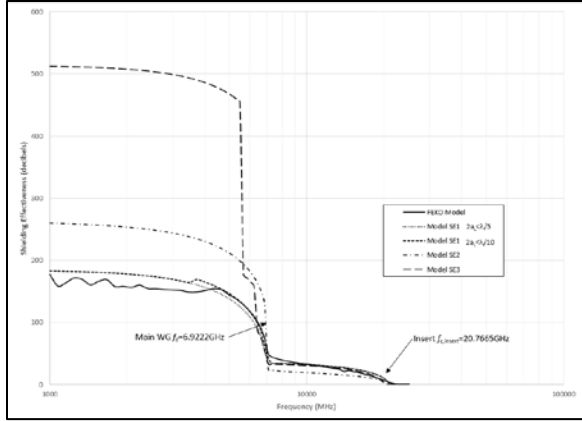
Figure 6 Comparison of SE_n, theoretical vs. results obtained using FEKO

Below approximately 6 GHz, the SE values obtained from the models vary widely from each other and the FEKO simulation results; however, at higher frequencies the general shape of all SE curves (theoretical vs. simulation) is comparable. Examination of the error between the various theoretical models and the FEKO results is shown in Table 4 for frequencies above the cutoff frequency f_c of the main waveguide.

Table 4 Average error and standard deviation of error, theoretical models vs. FEKO results, $f > f_c$

Model	Average Error ($\bar{x}$, dB)	Standard Deviation of Error (σ, dB)
SE$_1$ ($\lambda/10$)	-0.10	4.83
SE$_1$ ($\lambda/5$)	-0.35	4.23
SE$_2$ (Chen)	9.79	7.02
SE$_3$ (Lee)	2.31	4.47

The SE$_1$ model, based on a single honeycomb insert, followed the criteria of equation (19) i.e., equation (18) was applied at frequencies where the diameter of the waveguide was less than $1/10\lambda$. The SE$_1$ model was then modified to examine the effect of equation (18) up to frequencies where the diameter was less than $1/5$ λ. This model produced the lowest average error compared to the results of the FEKO simulation.

The SE$_2$ model, based on a honeycomb insert with multiple apertures, had the highest average error and error standard deviation of all models. The accuracy of equation (26) is dependent on the angle of incidence θ of the electromagnetic wave with respect to the normal at the boundary formed by the face of the insert. At frequencies lower than 8.021GHz, $\theta > 60°$. If these frequencies are excluded from the calculation of average error and error standard deviation, the values are reduced to 8.24 dB and 5.85 dB, respectively.

The SE$_3$ model, based on a single honeycomb insert, demonstrates a sensitivity to the value of the angle of incidence θ below f_c because of the dependency of the cosine term on θ in the logarithm in equation (27). This also holds true for equation (26) in the SE$_2$ model. If the condition $\theta < 90°$ is enforced for SE$_2$, and the second and third terms of SE$_3$ are eliminated, the behavior of all models is similar below f_c. This is shown in Figure 7.
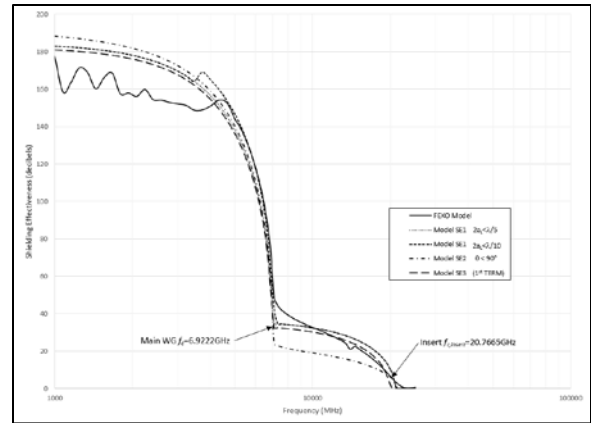

Figure 7 Comparison of SE_n, theoretical with modified conditions vs. results obtained using FEKO

CONCLUSIONS

Prior work has provided several formulas which may be used to estimate the SE of a waveguide, with no one complete model presented for a waveguide with a honeycomb insert. This paper has presented several potential models for a waveguide with an insert intended to increase the cutoff frequency. Consideration of the mathematical behavior of any particular model developed for this purpose must be taken into consideration.

It has also been shown the minimum number of inserts required to maintain a desired SE for a given waveguide may be calculated based on the dielectric constant of the coolant to be passed through the waveguide. The number of inserts, along with the different models presented, may be used to provide a conservative estimate of the SE of the required configuration for a waveguide with honeycomb insert.

REFERENCES

[1] K. Kelly, T. Abraham, K. Bennion, D. Bharathan, S. Narumanchi and M. O'Keefe, "Assessment of Thermal Control Technologies for Cooling Electric Vehicle Power

Electronics," in *23rd International Electric Vehicle Symposium (EVS-23)*, Anaheim, December 2-5, 2007.

[2] K. Cobb, "Burst of Power," *Accelerate,* pp. 8-11, March 2014.

[3] S. C. Mohapatra, "An Overview of Liquid Coolants for Electronics Cooling," 1 5 2006. [Online]. Available: http://www.electronics-cooling.com/2006/05/an-overview-of-liquid-coolants-for-electronics-cooling/. [Accessed 18 4 2016].

[4] U.S. Department of Defense, *Interface Standard: Requirements for the Control of Electromagnetic Interference Characteristics from Subsystems and Equipment,* 11 December 2015. (MIL-STD-461G).

[5] Department of Defense, *Electromagnetic Environmental Effects Requirements for Systems,* 01 December 2011. (MIL-STD-464C).

[6] C.-C. Chen, "Transmission of Microwave Through Perforated Flat Plates of Finite Thickness," *IEEE Transactions on Microwave Theory and Techniques,* Vols. MTT-21, no. 1, pp. 1-6, January 1973.

[7] M. K. McInerney, S. Ray, R. McCormack, S. Castillo and R. Mittra, "The Effect of Fluids on Waveguides Below Cutoff Penetrations as Related to Electromagnetic Shielding Effectiveness," Champaign, 1984.

[8] L. H. Hemming, "Applying the Waveguide Below Cut-Off Principle to Shielded Enclosure Design," in *IEEE International Symposium on Electromagnetic Compatibility*, Anaheim, 1992.

[9] K.-W. Lee, Y.-C. Cheong, I.-P. Hong and J.-G. Yook, "Design Equation of Shielding Effectiveness of Honeycomb," in *Proceedings of ISAP2005*, Seoul, 2005.

[10] ETS-LINDGREN, "Waveguide Feed-through (Pipe Penetrations) for Industrial Shielding," November 2008. [Online]. Available: http://www.ets-

lindgren.com/pdf/iWaveGuidePipePen.pdf. [Accessed 10 May 2016].

[11] *IEEE Standard Method for Measuring the Effectiveness of Electromagnetic Shielding Enclosures,* IEEE Standard 299, 2006.

[12] C. A. Balanis, Advanced Engineering Electromagnetics, Hoboken, NJ: John Wiley & Sons, 2012.

[13] W. H. Beyer, CRC Handbook of Mathematical Tables, 26 ed., Boca Raton, FL: CRC Press, 1981.

[14] G. G. Medveczky and T. Dickten, "High Quality Shielding with Predictable and Verifiable Effectiveness," *IEEE,* pp. 565-570, 1999.

[15] F. Choubani, J. David and N. E. Mastorakis, "Experiment on the Shielding by Hollow Conducting Tubes," *IEEE Transactions on Electromagnetic Compatibility,* vol. 48, no. 2, pp. 342-347, May 2006.

[16] D. R. Lide, "CRC Handbook of Chemistry and Physics," vol. 87, 2007.

[17] K. L. Kaiser, Electromagnetic Shielding, Boca Raton: CRC Press, 2006.

[18] C. R. Paul, Introduction to Electromagnetic Compatibility, K. Chang, Ed., New York: John Wiley & Sons, 1992.

[19] W. A. Bereuter and D. C. Chang, "Shielding Effectiveness of Metallic Honeycombs," *IEEE Transactions on Electromagnetic Compatibility,* Vols. EMC-24, no. 1, pp. 58-61, February 1982.

[20] Altair, FEKO Training Class (Suite 7.0) Course Notes, Troy, Michigan: Altair, 2015.

[21] R. L. Graham, B. D. Lubachevsky, K. J. Nurmela and P. R. J. Östergard, "Dense packings of congruent circles in a circle," *Discrete Mathematics,* vol. 181, pp. 139-154, 1998.